

# Development of an Efficient Three-Dimensional Optics Code

M. Nakano\* and Y. Arakawa†

The University of Tokyo

Hongo 7-3-1, Bunkyo-ku, 113 Japan

## Abstract

An efficient three-dimensional optics code has been developed for ion thruster research. The characteristic of the code is that one can calculate three-dimensional ion optics within a reasonable calculation time. The code employs a method that discharge plasma and ion sheath is divided self-consistently by the emission surface which helps avoid time-consuming calculation of the discharge plasma. The code also uses a view factor model to count charge-exchange ions due to residual neutrals to simulate ground-based test conditions. Several calculations were conducted on beam divergence and deflection characteristics and charge-exchange grid erosion in order to verify the code. Calculation results show that beam divergence angles agreed well with experiment data both for two-grid and three-grid systems and beam deflection angle for grid offset case agreed to the one predicted from linear optics theory. Calculations with charge-exchange reactions predicted fairly well values with experiment data for the accelerator impingement current and reasonably good values for the accelerator grid erosion rate. All calculations were done at practically low calculation cost: a typical calculation took less than an hour on a DEC Alpha workstation with 15 Mbytes of memory usage.

## Nomenclature

$a$	=	constant appeared on Eq. (9)
$b$	=	constant appeared on Eq. (9)
$e$	=	electron charge
$f$	=	view factor

$J$	=	beam current
$J_a$	=	accelerator beam current
$k$	=	Boltzmann constant
$l_e$	=	effective acceleration length
$M$	=	ion mass
$m$	=	electron mass
$n_e$	=	electron density
$n_i$	=	ion density
$n_n$	=	neutral atom density
NP/H	=	normalized perveance per hole
$P$	=	probability of charge exchange reaction
$\bar{P}$	=	normalized perveance
$R$	=	net to total voltage ratio
$T_e$	=	electron temperature
$V$	=	total voltage applied between screen and accelerator grids
$V_d$	=	discharge voltage
$v_i$	=	ion beam velocity
$\delta$	=	deflection angle
$\epsilon$	=	permittivity in free space
$\epsilon$	=	displacement of a grid
$\eta_u$	=	propellant utilization efficiency
$\phi$	=	electrostatic potential
$\sigma$	=	charge exchange cross section
$\tau$	=	transit time

## Introduction

Since an ion thruster system is now on the stage of practical application to space activities, great interest in ion thruster research has been focused on lifetime problems, especially on grid erosion issues. In this circumstances, ion beam simulation has gained an increased attention since experimental study on lifetime problems

\*Graduate Student, Department of Aeronautics and Astronautics, University of Tokyo.

†Professor, Department of Aeronautics and Astronautics, University of Tokyo, Member AIAA/JSASS.

is really costly. Several two-dimensional axisymmetric models have been constructed to simulate ion beam optics.<sup>1,2,3</sup> These two-dimensional models are very useful in lifetime estimation of a three-grid system since grid erosion occurs in the circumference of an accelerator and decelerator grid hole.

However, in a two-grid system, grid erosion occurs severely on the downstream surface of the accelerator grid and forms well-known pits & grooves pattern. Peng et al.<sup>4</sup> developed a three-dimensional particle simulation code to estimate grid erosion. The code predicted grid erosion well, however, the particle simulation technique requires too huge computation power to make parametric study possible on each extraction grid set. Therefore, efficient three-dimensional optics codes are necessary for ion thruster research.

In this study, an efficient three-dimensional optics code is presented. The code introduced the emission surface which made avoid calculation in the discharge plasma and dramatically reduced computation cost with success. The code also incorporates a view factor model<sup>5</sup> to include residual neutral effect for ground-based test condition. Calculations for beam divergence and deflection characteristics and grid erosion due to charge-exchange are presented in order to verify the code. The calculation results show that the code predicted beam divergence and deflection characteristics very well. The calculated grid erosion rate agreed to the experiment data to a reasonably good accuracy. All calculations were done at practically low calculation cost.

## Simulation Model

The optics code presented here consists of three parts: ion beam trajectory calculation, electrostatic potential calculation, and neutral atom density and charge-exchange ion trajectory calculations (if necessary).

A sketch of the computational domain is in Fig. 1. Calculations are done on a single-aperture grid set. The domain is divided by a surface (called the "emission surface" in the following,) where beams start their trajectories. The emission surface is determined self-consistently in such a way that the ion saturation current density of the plasma is equal to the space-charge limited current density at the emission surface.<sup>6</sup>

In the ion beam trajectory calculation, ions are considered single-charged. They are injected from the emis-

sion surface with the Bohm velocity and accelerated by the gradient of potential obeying the equation of motion

$$M \frac{dv_i}{dt} = -e \nabla \phi \quad (1)$$

The trajectories of these ions are followed until they escape from the computational domain or impinge on the grid.

In the electrostatic potential calculation, potentials are calculated from the Poisson's equation

$$\nabla^2 \phi = -\frac{e}{\epsilon} n_i \quad (2)$$

In the downstream region where neutralization process occurs, neutralizing electrons are added and Eq.(2) is replaced by

$$\nabla^2 \phi = -\frac{e}{\epsilon} (n_i - n_e) \quad (3)$$

where the density of neutralizing electrons is given by

$$n_e = n_{e0} \exp\left(\frac{e\phi}{kT_e}\right) \quad (4)$$

The potential of the emission surface  $\phi_E$  is given by<sup>7</sup>

$$\begin{aligned} \phi_E &= \phi_S + V_d - \frac{kT_e}{e} \log\left\{\frac{1}{0.6888\sqrt{\pi}} \left(\frac{M}{m}\right)^{1/2}\right\} \\ &- 0.854 \frac{kT_e}{e} \end{aligned} \quad (5)$$

where  $\phi_S$  is a screen grid potential.

In the downstream region, a neutralizing surface is placed at the distance  $l_n$  downstream of the accelerator grid. All charge-exchange ions created upstream of the neutralizing surface (in the potential well) are drawn to the grid. The distance to the surface is calculated by the Kerslake model.<sup>8</sup>

$$l_n = \sqrt{\frac{1 + 3R^{0.5} - 4R^{1.5}}{\bar{P}}} l_e \quad (6)$$

The boundaries on the emission surface, screen, accelerator and decelerator grid are given their potential values. The other boundaries are given by the natural boundary condition. The space charge density downstream of the neutralizing surface is set zero.

In the neutral atom density calculation, neutral atom density is computed by a rarefied gas flow model based on the Monte Carlo method in order to calculate the production rate of charge-exchange ions. Neutral particles start from the boundary far upstream of the screen grid with their velocities having Maxwellian distribution at the wall temperature of a discharge chamber.

Neutral particles reached on the grid are reflected back to the computation domain following the cosine law (reflection is assumed to be diffuse). No collisions between neutrals are considered since the mean free path of the neutrals is much longer than the size of a grid set. The neutral atom flux is determined so as to satisfy the following condition.

$$\Gamma_n = \frac{(1 - \eta_u) J}{e\eta_u} \quad (7)$$

Residual neutrals in ground-based tests are assumed to be isotropic and constant neutral density value is added to the neutral density distribution obtained by the above procedure.

In the charge-exchange ion trajectory calculation, firstly, the charge-exchange ion production rate is calculated. The possibility of charge exchange reaction in a prescribed length is calculated by Eq. (8) using charge exchange cross section, neutral atom density, ion beam velocity, and ion beam transit time.

$$P = \exp(-n_n \sigma v_i \tau) \quad (8)$$

The charge exchange cross sections used in the optics code are obtained from Ref.[9] and incorporated using the following relationship.

$$\sigma^{1/2} = a - b \log v_i \quad (9)$$

The amount of charge-exchange ions is calculated by the ion beam current and the charge-exchange reaction rate. The charge-exchange ions start from the point where they are created with a thermal velocity of neutrals, and their trajectories are followed until they collide with a grid or escape from the computational domain.

The charge-exchange ions created by the collision between ion beams and residual neutrals have a chance of being drawn into the grid even if they are created far downstream of the neutralizing surface. If the velocity of the residual neutrals is assumed to be isotropic, the amount of charge-exchange ions drawn into the accelerator grid can be calculated by the following view factor model<sup>5</sup>

$$J_{cex} = \int J(z) \sigma(z) n(z) f(r, z) dz \quad (10)$$

where the view factor is evaluated at each point of the downstream region. The charge-exchange ions created downstream of the neutralizing surface are injected from

the neutralizing surface and their trajectories are calculated. The erosion rate of the grid is calculated by the yield model<sup>10</sup> and no dependence on the angle of incidence of the ions is considered.

## Calculation Procedure

The block diagram of the optics code is in the Fig. 2. Firstly, the geometric and operating parameters are given. The geometric data consist of the aperture diameter and width of the screen, accelerator and decelerator grids, and the separation distance of these grids. To simulate ground-based test conditions, the beam diameter of a thruster is required for calculating the amount of charge-exchange ions created far downstream of the neutralizing surface. The operating parameters consist of normalized perveance per hole (NP/H) or beam current density, discharge voltage, propellant utilization efficiency and residual neutral atom density.

In the main part of the procedure, the position of the emission surface is assumed and the electrostatic potentials are calculated by solving the Laplace equation. The finite element method is used to determine the potentials. Then ion beams start from the emission surface and their trajectories are followed. The space charge density is calculated for each element by adding the charge of each ion beam passing through it. After space charge density profile is obtained, the Poisson's equation is solved to yield potentials and the new emission surface is determined. These steps are repeated until the solution converges to within a predetermined accuracy.

In the calculation with charge-exchange reactions, neutral atom density and charge-exchange ion beam calculation blocks are added to the block diagram.

## Results and Discussion

### Beam Divergence and Deflection Characteristics

Calculations were conducted on the beam divergence and deflection characteristics on the grid set on Table 1 to investigate the validity of the emission surface model.

Figures 3 and 4 show beam divergence angles of the two-grid and three-grid systems, where the beam divergence angle was defined by the half angle of the cone enclosing 95 % of the integrated beam current downstream of each grid set. For comparison, the experimental data

Table 1: Extraction grid system for calculations

Geometric & Operating Parameters	Two-Grid System	Three-Grid System
Screen hole dia.	2.1 mm	2.1 mm
Accel hole dia.	1.3 mm	1.3 mm
Decel hole dia.	—	1.7 mm
Screen grid thickness	0.4 mm	0.4 mm
Accel grid thickness	0.8 mm	0.8 mm
Decel grid thickness	—	0.8 mm
Screen-to-accel grid gap	1.0 mm	1.0 mm
Accel-to-decel grid gap	—	1.0 mm
Total acceleration voltage	1100 V	1100 V
Net-to-total voltage ratio	0.7	0.3

measured by Aston<sup>11,12</sup> are shown. In both the grid systems, the calculated beam divergence angles agreed well with the experimental data.

In Figure 5, a plot of deflection angle against grid offset angle is represented for the two-grid system on Table 1 where the grid offset angle  $\delta$  was defined in terms of the grid displacement  $\epsilon$  by the equation

$$\delta = \tan^{-1} \frac{\epsilon}{l_g + t_s} \quad (11)$$

where  $l_g$  is a screen-to-accel grid gap and  $t_s$  is a screen grid thickness. To check validity, a line obtained from linear optics theory is also on the figure. In all the range, the code did good predictions of beam deflection angle.

These calculations show that the emission surface is a useful model for ion beam optics which makes avoid time-consuming calculation in the discharge plasma without spoiling beam divergence and beam deflection characteristics of the ion beam optics.

### Charge-Exchange Grid Erosion

Calculations including charge-exchange collisions have been conducted for the LeRC<sup>13</sup> and JPL<sup>14</sup> test cases. The accelerator grid impingement current and the grid erosion rate for these tests were calculated and compared to the experiment data. Calculations for space-based operating condition were also conducted and their results were compared to the PIC simulation results by Peng et al.<sup>4</sup>

The grid used in these experiments was a two-grid type with an effective beam diameter 28.2 cm.<sup>13,14</sup> The screen grid was 1.9 mm aperture diameter and its thickness was 0.36 mm. The accelerator grid diameter was 1.1 mm and its thickness was 0.36 mm. The separa-

Table 2: Accelerator grid current and grid mass loss

		LeRC	JPL
$J_a/J$	Exp. <sup>13,14</sup>	0.55%	1.25%
	PIC <sup>4</sup>	0.55*%	1.25*%
	This study	0.631(0.094+)%	1.15(0.116+)%
$M_{\text{loss}}$	Exp. <sup>13,14</sup>	17.2 g	44.8 g
	PIC <sup>4</sup>	23.2 (3.7+) g	55.16 (3.35+) g
	This study	27.7 (1.34+) g	49.9 (1.62+) g

\*: using experiment data as an input parameter

+: under space-based operating condition

tion distance of the grids was 0.76 mm. The LeRC test used xenon as propellant and the assumed operating conditions for the calculation were: the total acceleration voltage 1800 V, the accelerator voltage -330 V, and the beam current 3.2 A with 90 % propellant utilization efficiency and the discharge voltage 28 V. The JPL test used krypton as propellant and the assumed operating conditions for the calculation were: the total acceleration voltage 1520 V, the accelerator voltage -500 V, and the beam current 2.8 A with 82 % propellant utilization efficiency and the discharge voltage 40 V. The chamber pressure for the LeRC case was assumed to be  $1.7 \times 10^{-3}$  Pascal and  $3 \times 10^{-5}$  Torr for the JPL case. Other data were set so as to give the same operating conditions.

Shown on Table 2 are the accelerator grid impingement current to beam current ratio and the accelerator grid mass loss for the experiments,<sup>13,14</sup> the PIC simulation<sup>4</sup> and the simulation results of this code respectively.

The calculated accelerator grid impingement current to beam current ratio for the LeRC case was 0.631 % and agreed well with the experiment data to within an accuracy of 15 %. The calculated accelerator grid impingement current to beam current ratio without residual neutrals (assuming space-based operating condition) was about 15 % of the impingement current ratio for ground-based test condition. These facts suggest that most of the charge-exchange ions impinged on the grid in the test were produced from residual neutrals and its amount can be estimated by a simple view factor model assuming isotropic velocity distribution of residual neutrals. The PIC code<sup>4</sup> used the accelerator grid impingement current as an input parameter, however, by using the view factor model there is no need for one to use the accelerator grid impingement current for the

input parameter of the simulation.

The accelerator grid mass loss for ground-based test condition was 27.7 g in the calculation which is 60% larger than the one in the experiment. Considering a good agreement of the accelerator grid impingement current to beam current ratio, this difference can be attributable to the difference of the sputter yield of the simulation and the one in the experiment.

The calculated grid mass loss for space-based operating condition is also on Table 2. The calculated grid mass loss for space-based operating condition was 1.34 g and an order of magnitude smaller than the grid mass loss for ground-based test condition. This corresponds to the an order of magnitude smaller accelerator grid impingement current for space-based operating condition. It should be noted that the ratio of the grid mass loss to the accelerator impingement current is smaller for space-based operating condition than the one for ground-based test condition. This is explained by the location at which charge-exchange ions were created. Most of the charge-exchange ions impinged on the accelerator grid for ground-based test condition were created far downstream of the accelerator grid and they impinged on it with the energy corresponding to accelerator grid potential, however, for space-based operating condition no charge-exchange ions created downstream of the neutralizing surface were drawn back to the accelerator grid and charge-exchange ions created upstream of the neutralizing surface impinged on the grid with smaller energy corresponding to the potential difference between accelerator grid potential and the potential at which they were created.

In comparing this simulation result to the PIC simulation in Ref.[4], the value is one third to the one obtained by the PIC simulation (the simulation results for JPL case show the same trend.) The most probable explanation of this difference can be given by the length of the downstream computational domain. The code in this study uses the Kerslake model to determine the length to the neutralizing surface, which tends to be smaller than other simulation models. Since the number of charge-exchange ions impinging on the grid depends on the downstream volume in which charge-exchange reactions occur, the code tends to predict smaller erosion rate. This is a qualitative explanation and it must be explained quantitatively, however, no quantitative explanation is possible since the exact downstream length

is not mentioned in Ref. [4]. Off course, other explanations are possible, however, the above discussion is most probable to explain the difference of the grid mass loss.

Figure 6 shows a calculated erosion pattern on the downstream surface of the accelerator grid for ground-based test condition. It clearly shows a pits & grooves pattern those seen by endurance tests. Shown in Fig. 7 is a calculated erosion pattern on the downstream surface of the accelerator grid for space-based operating condition. It shows a flat and less clear erosion pattern, and no pits & grooves pattern appeared. These two patterns and the smaller accelerator impingement current for space-based operating condition suggest that the pits & grooves pattern erosion appeared due to the facility effect.

The accelerator grid impingement current and accelerator grid mass loss for the JPL case are also presented on Table 2. The accelerator grid impingement current to beam current ratio for ground-based test condition was 1.15% in the calculation and 1.25% in the experiment. This again shows a very good agreement. The accelerator grid mass loss for ground-based test condition was calculated 49.9 g which agreed with the experimental data with good accuracy (44.8 g grid mass loss in the experiment,<sup>14</sup>) however, grid mass loss was again overestimated. The calculated accelerator grid impingement current for space-based operating condition was about 10% of the impingement current for ground-based test condition. The calculated grid mass loss for space-based operating condition was 1.62 g and is an order of magnitude smaller than the calculated value for ground-based test condition. The grid mass loss for space-based operating condition is one half of the PIC simulation result in Ref.[4]. The explanation of the differences of the calculated values to the experiment data<sup>14</sup> and the PIC simulation results<sup>4</sup> can be given by the same discussion for the LeRC case.

### Efficiency of the Code

All calculations presented in this paper were performed on a DEC Alpha workstation (CPU Alpha 21164A 500MHz). Typical calculation time for beam divergence and beam deflection characteristics took about 20 minutes on a computational grid of about 5000 elements. Calculation time including charge-exchange reactions took about 40 minutes. The calculation time

doubled compared to the no charge-exchange reaction calculation, however, the half of the calculation time was spent on the neutral atom density calculation of the 3-D Monte Carlo method. Therefore in a parametric study using the same grid set calculation time can be reduced to 20 minutes once after the neutral atom density distribution profile is obtained. The use of two-dimensional axisymmetric model for neutral density calculation is expected to reduce computation time.

Memory usage in the calculations with and without charge-exchange reactions was less than 15 Mbytes, which was required for matrix operations in the electrostatic potential calculation. Much smaller memory was needed for the ion beam calculation.

These computational characteristics of the code make parametric study possible and special computation environment will not be necessary.

### Summary

An efficient three-dimensional optics code has been developed for ion thruster research. The code incorporates the emission surface and view factor models to simulate three-dimensional ion optics efficiently.

Numerical examples show that the code calculated beam divergence and deflection characteristics to a good accuracy. In the charge-exchange grid erosion calculations, the view factor model yielded the accelerator impingement current which agreed well with the experimental data, however, the model overestimated accelerator grid mass loss. This suggests that more refined sputter yield models are necessary. For space-based operating condition, the calculated erosion rate was an order of magnitude smaller than the value for ground-based test condition and the calculated erosion pattern on the downstream surface of the accelerator grid was flat. These calculation results suggest that pits & grooves pattern erosion is due to the facility effect. The calculated erosion rate for space-based operating condition was the same order of magnitude to the one by the PIC simulation<sup>4</sup> and the difference of the rates may be explained by the length of the downstream computation domain.

The code ran three-dimensional calculations in a reasonable computation time and memory usage. From these results, it is concluded that this code is an efficient and useful tool for estimating ion beam characteristics

and grid erosion due to charge-exchange, and helps ion thruster research.

### Reference

1. R. A. Bond and P. M. Latham, "Extraction System Design and Modeling Using Computer Codes," IEPC-93-179, Seattle, Sep. 1993.
2. R. A. Bond and P. M. Latham, "Ion Thruster Extraction Grid Design and Erosion Modeling using Computer Simulation," AIAA 95-2923, San Diego, July 1995.
3. T. Shiraishi, H. Kuninaka, S. Satori and K. Kuriki, "Numerical Simulation of Grid Erosion for Ion Thruster," Proceedings of the 24th International Electric Propulsion Conference, Vol.1, pp.586-594.
4. X. Peng, W. M. Ruyten and K. Dennis, "Charge-Exchange Grid Erosion Study for Ground-Based and Space-Based Operations of Ion thrusters," IEPC-93-173, Seattle, WA, Sep., 1993.
5. J. M. Monheiser and P. J. Wilbur, "Effects of Design and Operating Conditions on Accelerator-Grid Impingement Current," IEPC-93-174, Seattle, Sep. 1993.
6. Y. Aarakawa and M. Nakano, "An Efficient Three-Dimensional Optics Code for Ion Thruster Research", 32nd joint Propulsion Conference, FL, July 1996.
7. S. A. Self, "Exact Solution for the Collisionless Plasma-Sheath Equation," The Physics of Fluids, Vol.6, No.12, 1762-1768.
8. W. R. Kerslake, "Charge-Exchange Effects on the Accelerator Impingement of an Electron-Bombardment Ion Rocket," NASA TN D-1657, May 1963.
9. J. B. Hasted, "Physics of Atomic Collision," 1964.
10. D. Rosenberg and G. K. Wehner, "Sputtering Yields for Low Energy He<sup>+</sup>, Kr<sup>+</sup>, and Xe<sup>+</sup> Ion Bombardment," Journal of Applied Physics, Vol. 33, No.5, 1962.

11. G. Aston, H. R. Kaufman and P. J. Wilbur, "Ion Beam Divergence Characteristics of Two-Grid Accelerator Systems," AIAA Journal, Vol.16, No.5, 1978, pp.516-524.
12. G. Aston and H. R. Kaufman, "Ion Beam Divergence Characteristics of Three-Grid Ion Accelerator Systems," AIAA Journal, Vol.17, No.1, 1979, pp.64-70.
13. M. J. Patterson and R. V. Timothy, "5 kW Xenon Ion Thruster Lifetest", AIAA 90-2543, Orlando, FL, July, 1990.
14. J. R. Brophy, J. E. Polk and L. C. Pless, "Test-to-Failure of a Two-Grid, 30-cm-dia. Ion Accelerator System," IEPC-93-172, Seattle, WA, Sep., 1993.

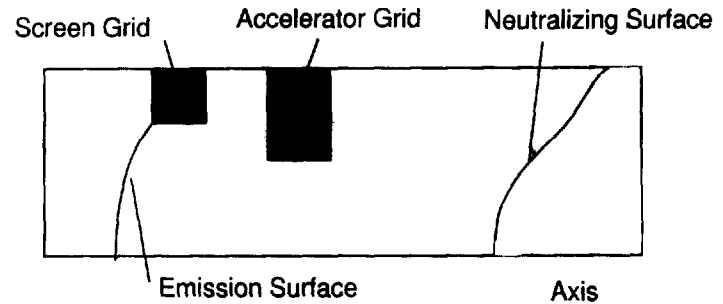


Figure 1: Computational domain

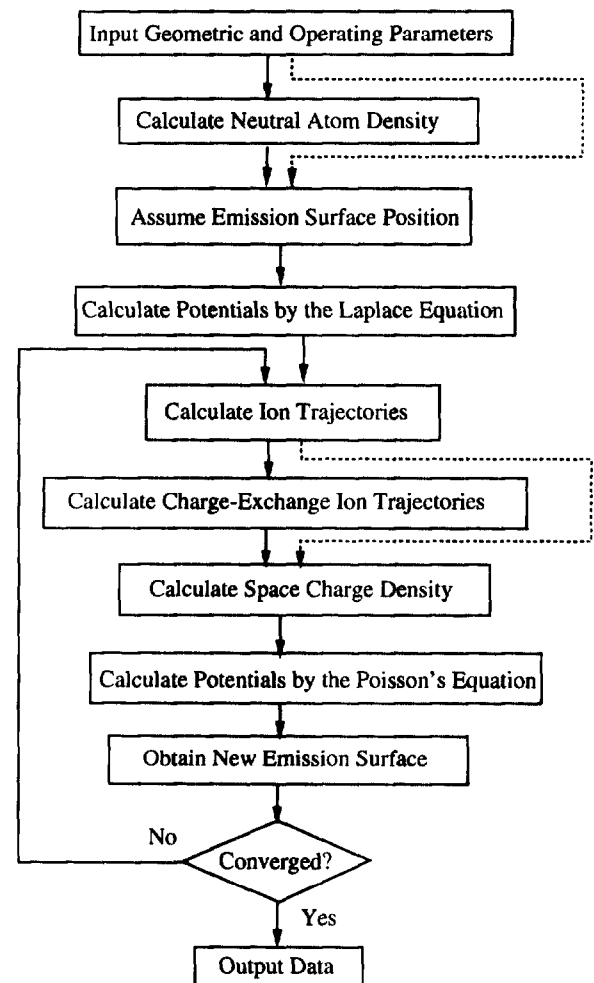


Figure 2: Block diagram of the code

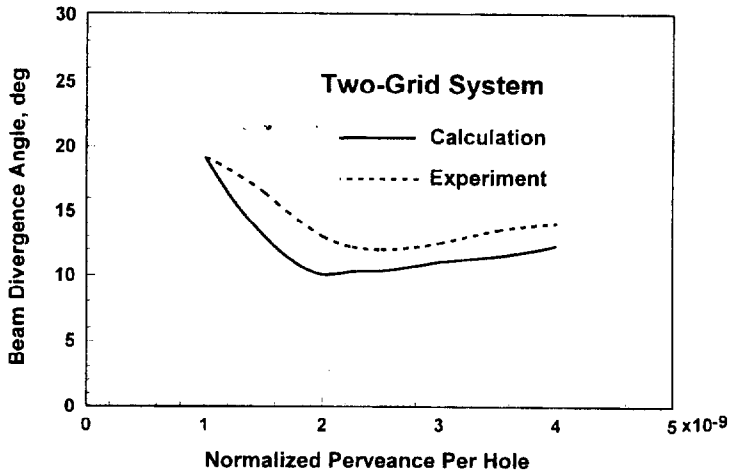


Figure 3: Beam divergence characteristics for a two-grid system

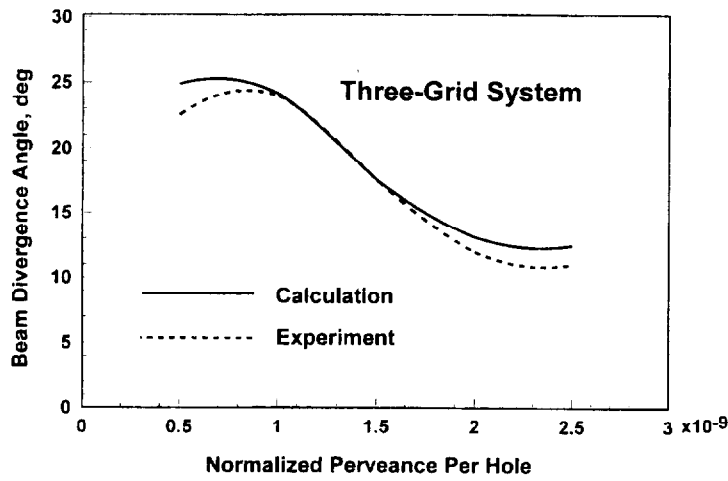


Figure 4: Beam divergence characteristics for a three-grid system

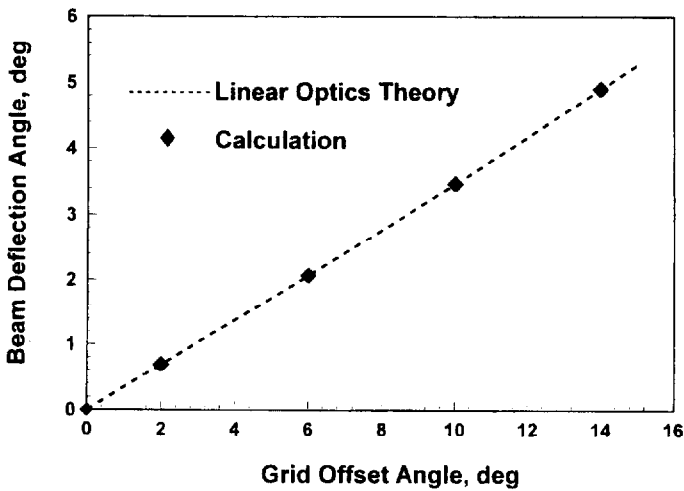


Figure 5: Beam deflection angle against grid offset angle

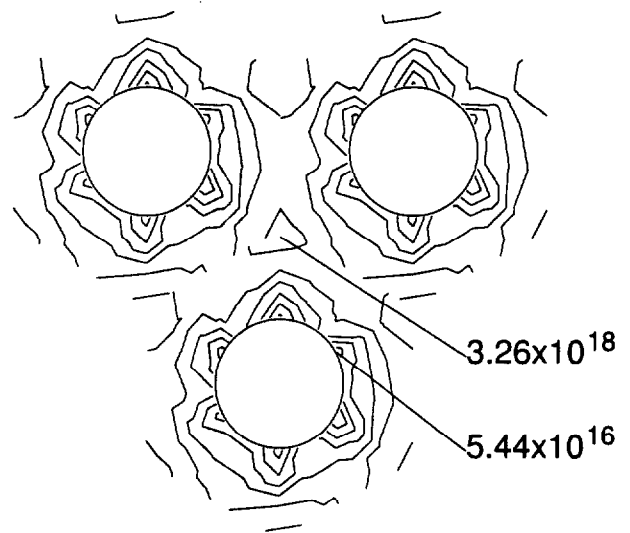


Figure 6: Erosion pattern on the downstream surface of the accelerator grid for ground-based test condition (values are number of sputtered atoms per square meters per second.)

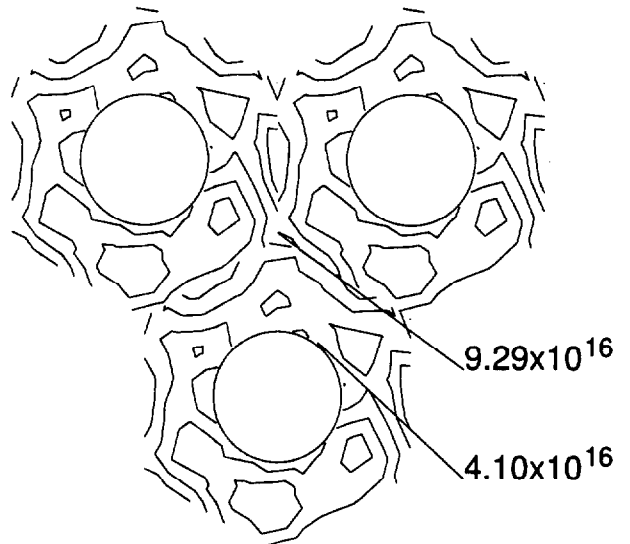


Figure 7: Erosion pattern on the downstream surface of the accelerator grid for space-based operating condition (values are number of sputtered atoms per square meters per second.)